JOURNAL OF CATALYSIS 83, 323–335 (1983)

Temperature-Programmed Reduction. Parametric Sensitivity and Estimation of Kinetic Parameters

DANIELE A. M. MONTI AND ALFONS BAIKER[1]

Department of Industrial and Engineering Chemistry, Swiss Federal Institute of Technology (ETH), CH-8092 Zurich, Switzerland

Received January 24, 1983; revised May 13, 1983

The influence of the different experimental operating variables used in temperature-programmed reduction (TPR) measurements on the reduction profiles has been studied using the reduction of nickel oxide as an example. The temperature range and the shape of the resulting TPR profiles were markedly affected by the experimental conditions. A characteristic number, K, is defined to aid in selecting the values for the operating variables which should be chosen in order to obtain optimum reduction profiles. The number relates the heating rate, hydrogen concentration, total flow rate, and the amount of reducible sample in such a way that the operating variables can easily be adjusted. Upper and lower limits are proposed for this characteristic number, and the influence of its variation on the sensitivity of the TPR method is discussed. Different methods for estimating the kinetic parameters of the reduction of nickel oxide from TPR experiments are compared. A peak shape analysis leads to narrower confidence limits for the kinetic parameters than an estimation based on the shift of the temperature of the maximum reduction rate measured for different heating rates. Simple criteria are proposed to check whether TPR measurements are free from mass transfer limitations.

INTRODUCTION

Temperature-programmed reduction (TPR) has gained increasing importance for the characterization of catalysts since its first application by Robertson *et al.* (*1*). The TPR technique has been applied successfully to study the influence of support materials (*2, 3*), of pretreatment procedures (*4, 5*), and of application of promoters (*6, 7*) on the reducibility of the catalyst surface. An essential extension of the TPR technique was obtained by mass analysis of the gases produced during the reduction (*8*). A comprehensive review on the basic concepts of the TPR technique, including many experimental profiles, has recently been reported (*9*).

However, the parametric sensitivity of the TPR technique as well as the quantitative evaluation of TPR data, has scarcely been discussed in the literature. Gentry *et al.* (*10*) studied the effect caused by variation of the experimental parameters on the temperature corresponding to the maximum hydrogen consumption rate for the reduction of copper ions in zeolites. They proposed a method to estimate the activation energy using profiles obtained with different heating rates. The influences of the hydrogen concentration of the hydrogen flow rate and of the amount of sample have also been discussed briefly by these authors.

For TPR measurements reported in the literature, the experimental conditions employed vary over a wide range. The reducing gas usually consists of a mixture of either hydrogen and nitrogen or hydrogen and argon. The reported hydrogen concentrations range from 3 to 15%; the flow rates from 0.16 to 1 cm^3 (NTP)/s, and the sample volumes from 10 to 500 μmol. A comparison of the results reported in the literature often becomes very difficult due to the fact that the reduction profiles are sensitive to the experimental conditions used. We feel that a first step to a better interpretation of

[1] To whom all correspondence should be addressed.

0021-9517/83 $3.00

TPR profiles can only be achieved if more is known about the parametric sensitivity of this technique.

This led us to study quantitatively the effects of the experimental parameters on the resulting TPR profiles using pure nickel oxide as an example. Methods for the estimation of the kinetic parameters of the reduction from experiments carried out with different heating rates and hydrogen concentrations are proposed. Confidence limits of the parameters obtained using the proposed estimation procedures are compared. Effects caused by varying the total flow rate and the sample volume are investigated and their impact on the sensitivity of the method are discussed. Finally, some criteria are given to estimate the influence of internal and external mass transfer limitations on TPR measurements.

EXPERIMENTAL

Sample Preparation and Characterization

Nickel oxide. Pure nickel oxide powder was prepared by a conventional precipitation method from the corresponding metal nitrate (Fluka AG) (*11*). The precipitate was first dried in air for 24 h at 380 K and subsequently calcined for 4 h at 670 K. The BET surface area measured by nitrogen adsorption was 50 m^2/g and the mean particle size determined by X-ray diffraction line broadening was 13.5 nm. After complete reduction of the metal at 550 K, the BET surface area was 11 m^2/g. Only NiO particles with diameters of less than 100 μm were used in the TPR experiments.

Supported copper oxide. This was prepared from copper nitrate (Fluka AG) and aluminum hydroxide (BDH Chemicals Ltd.) as described elsewhere (*12*). Physical properties of the solid after calcination at 890 K for 24 h are listed in Table 1.

TABLE 1

Properties of the Alumina-Supported Copper Oxide Catalyst

Metal loading, wt%	6.2
BET surface area, m^2/g	206
Specific pore volume, cm^3/g	0.44
Solid density, g/cm^3	3.4
Apparent density, g/cm^3	1.36
Mean pore radius, Å	43

Apparatus

The experimental arrangement employed for the TPR measurements is shown schematically in Fig. 1. The total flow rate and the hydrogen concentration could be varied independently. The flow rates of the hydrogen (99.999%, Sauerstoff- und Wasserstoffwerke AG, Luzern) and of the nitrogen (99.995%, same manufacturer) could be adjusted with an electronic thermal mass flow controller (Brooks Instruments, Model 5840). A temperature controller (Stanton Redcroft, LVP/CA40/R) was used to vary the temperature between 300 and 1200 K with linear heating rates. The quartz glass reactor was constructed according to the suggestions made by Cvetanović and Amenomiya (*13*). Special care was taken to minimize the volume of the tubing between the reactor and the detector and to minimize the relaxation time of the temperature measurement (*14*). The sensitivity of the hot wire detector (HWD, GowMac, Model 69-552) was determined for all experimental conditions used and the linearity of the output signal obtained with respect to the hydrogen concentration was checked.

Procedure

The general procedure can be divided into a pretreatment and a measuring step. All samples studied were first heated in dry nitrogen (1 cm^3 (NTP)/s) at 670 K for 1 h to eliminate traces of adsorbed water. The supported copper oxide was ground and fractions with mean particle radii of 75 to 350 μm were formed. The samples (0.4 g) were pretreated in the same way as the nickel oxide powder. After cooling to room temperature, the nitrogen was replaced by the reducing gas and the linear temperature program was started. The hydrogen con-

sumption rate and the temperature were simultaneously recorded as a function of time. Measured TPR peaks were usually characterized by the temperature corresponding to the maximum hydrogen consumption rate, T_M, and by the breath of the peaks at half maximum intensity, $B_{1/2}$.

NOMENCLATURE

Symbols

A	outer surface area of sample (cm^3)
c	current concentration of hydrogen at the reactor outlet ($\mu mol/cm^3$)
$\bar{c}$	mean hydrogen concentration; $(c + c_0)/2$ ($\mu mol/cm^3$)
c_s	hydrogen concentration at outer surface of a particle ($\mu mol/cm^3$)
D	diffusion coefficient (cm^2/s)
dn/dt	current hydrogen consumption rate ($\mu mol/s$)
E_A	apparent activation energy (kJ/mol)
k	rate constant for the reduction process (1/(mol · s))
k_0	preexponential factor (1/(mol · s))
k_f	fluid-solid mass transfer coefficient (cm/s)
K	characteristic number; $S_0/(c_0 \cdot V^*)$ (s)
Pe	Peclet number
R_p	particle radius (cm)
Re_p	Reynolds number
S	current amount of reducible species (μmol)
Sc	Schmidt number
Sh	Sherwood number
t	time (s)
T	current temperature of the sample (K)
V^*	total flow rate of the reducing gas (cm^3(NTP)/s)
V_c	sample volume (cm^3)
V_t	volume between reaction zone and detector (cm^3)

Greek symbols

β	heating rate (K/s)
ε	porosity of the sample bed
τ	relaxation time for temperature measurement (s)
Φ	dimensionless number, see Eq. (19)

Indices

M	index for maximum conditions
o	index for initial values of variables

DATA ANALYSIS

The reduction kinetics of a solid species S with hydrogen at constant temperature may be described (10) with:

$$\frac{dS}{dt} = \frac{dn}{dt} = -kS^q\bar{c}^m \tag{1}$$

where k is the rate constant, S the sample weight, and q and m are the reaction orders. Conversely to Gentry *et al.* (10) we use the mean hydrogen concentration, $\bar{c}$, between reactor inlet and outlet instead of the outlet concentration. The application of the mean concentration seems to be more appropriate because a differential reactor is considered. The hydrogen mass balance is then given by:

$$V^*c_0 = V^*c + kS^q\bar{c}^m \tag{2}$$

Taking into account a constant heating rate and that the temperature dependence of the rate constant obeys the Arrhenius law, we obtain

$$\frac{dT}{dt} = \beta \tag{3}$$

$$k = k_0 \exp(-E_A/RT) \tag{4}$$

With the simplifying assumption of first-order kinetics with respect to the solid and the hydrogen ($m = q = 1$) the combination of Eqs. (1)–(4) leads to the following correlation between the experimental (V^*, c_0, β, S) and the kinetic (k_0, E_A) parameters.

$$\frac{dS}{dT} = \frac{dn}{dT} = -\frac{2c_0V^*}{\beta}\left(\frac{1}{1 + \dfrac{2V^*}{Sk_0\exp\left(\dfrac{-E_A}{RT}\right)}}\right) \tag{5}$$

At the temperature of the maximum reduction rate, we can write:

$$\frac{d}{dT}\left(\frac{dS}{dT}\right) = \frac{d}{dT}\left(\frac{dn}{dT}\right) = 0 \tag{6}$$

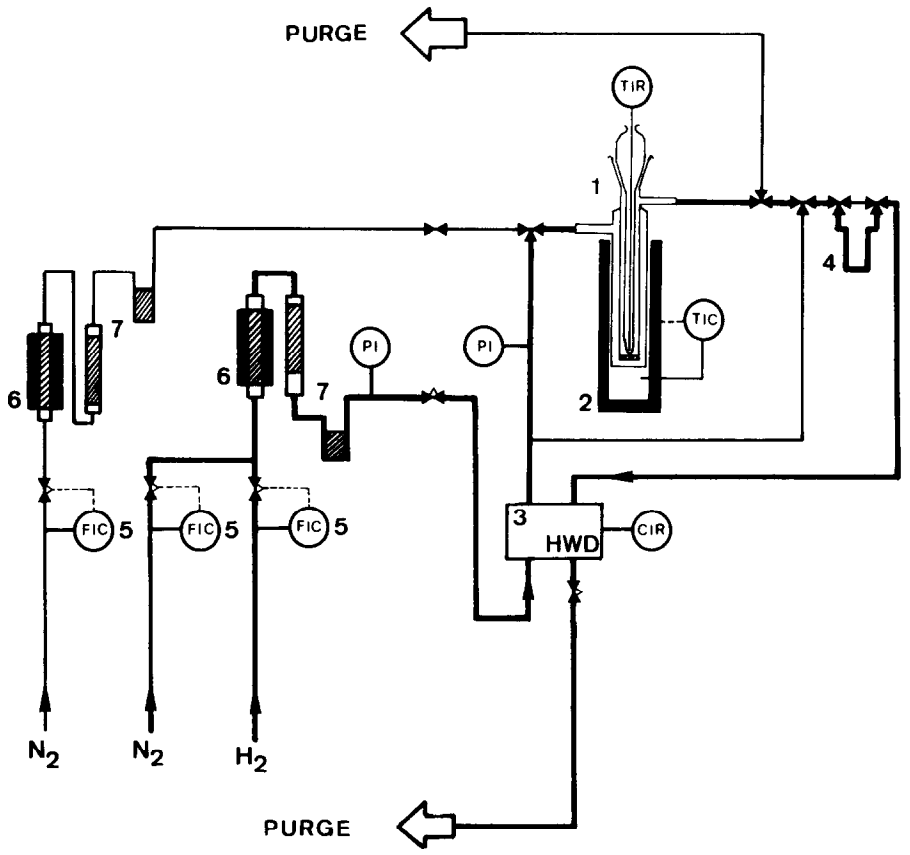

FIG. 1. Experimental arrangement used for the TPR measurements. (1) Reactor, (2) temperature controlled furnace, (3) hot wire detector, (4) cooling trap filled with glass spheres (195 K), (5) electronic mass flow controller, (6) copper-filled furnace (550 K), (7) molecular sieve packings (293 and 195 K). FIC, flow control; PI, pressure gauges; TIC, temperature control; TIR, temperature recording; CIR concentration recording.

With an analogous procedure as was applied earlier for the analysis of TPD profiles (*13*), the combination of Eq. (1) with $m = q = 1$ and Eq. (6) yields:

$$\frac{E_A}{RT_M^2} = \frac{k_0}{\beta}\bar{c}_M \exp\left(-\frac{E_A}{RT_M}\right) \qquad (7)$$

Taking logarithms and rearranging leads to the linear equation usually employed to estimate E_A and k_0:

$$\ln\frac{T_M^2\bar{c}_M}{\beta} = \frac{E_A}{RT_M} + \ln\frac{E_A}{Rk_0} \qquad (8)$$

By using the initial condition $S = S_0$ at $T = T_0$ and inserting values for the estimated kinetic parameters, numerical integration of Eq. (5) gives the relation between the current hydrogen consumption rate and the sample temperature. Both the sample temperature and the difference in inlet and outlet hydrogen concentration are expressed relative to their values at the peak maximum.

$$T_n = T/T_M \qquad (9)$$

$$c_n = (c_0 - c)/(c_0 - c_M) \qquad (10)$$

$$E_M = E_A/RT_M \qquad (11)$$

After numerical integration of Eq. (5) and standardization with Eqs. (9) and (10), it is possible to evaluate the normalized concentration C_n as a function of the normalized temperature T_n. Some illustrative plots of the normalized peak shapes are shown in

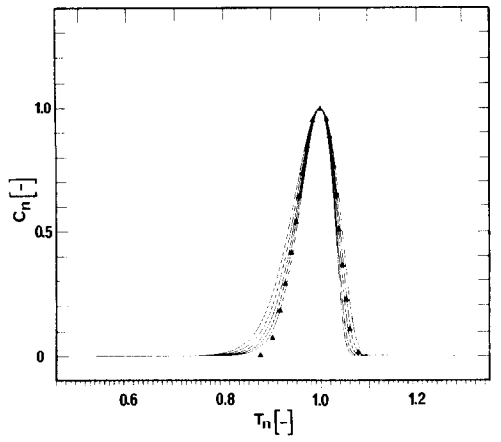

FIG. 2. Dimensionless TPR peak shape analysis for different values of E_M. The peaks become sharper with increasing E_M. E_M = 22.0, 24.4, 26.8, 29.2, 31.6.

Fig. 2. From these plots it emerges that the only parameter determining the peak shape is E_M, and that the asymmetric peaks become sharper as the value of E_M increases.

Using a computer program for the regression analysis of single- and multi-response algebraic and ordinary differential equation models (*15*), the estimation of k_0 and E_A can be carried out for each TPR profile. The computer program numerically integrated Eq. (5) and estimated values of k_0 and E_A to give the best fit of the theoretical curve to the measured TPR peak. Analysis of the peak shapes using the normalized variables C_n and T_n and estimation of the kinetic parameters by using a regression computer program have the advantage that only one accurately measured peak is needed for a preliminary quantitative description of the reduction kinetics. By applying numerical methods it is possible to develop the same kind of data analysis for more complex kinetic rate expressions.

RESULTS AND DISCUSSION

Influence on Reduction Profiles of Dispersion and Time Lag in the Temperature Measurement

To investigate the influence of dispersion caused by the tubing between the reactor and the detector, tracer experiments were performed. A special reactor system was designed which allowed injection of a small quantity of the tracer gas (He, 1 cm³ (NTP)) directly into the reactor. A Dirac delta-input signal of the nonadsorbable tracer was injected into the reducing gas mixture at a standard total flow rate of 1.25 cm³ (NTP)/s. The measured residence time distribution could be described satisfactory by a tanks-in-series model of 45 equally sized ideally mixed tank reactors with a mean residence time in each tank of 0.804 s.

$$f(t) = \frac{t^{N-1}\exp(-t/t_i)}{t_i^N(N-1)!} \qquad \begin{matrix} N = 45 \\ t_i = 0.804\ \text{s} \end{matrix} \tag{12}$$

An estimated axial Peclet number ($Pe = u \cdot L/D$) of 90 indicates a nearly Gaussian elution curve for the tracer response. From the shape of a TPR peak measured under appropriate experimental conditions, a standard deviation of 2 min was estimated. The test peak was described by a Gaussian distribution.

$$g_{in}(t) = \frac{600}{\sqrt{2\pi}\,\sigma}\exp\left(-1/2\left(\frac{t-\mu}{\sigma}\right)^2\right) \tag{13}$$

$$(\mu = 900\ \text{s};\ \sigma = 120\ \text{s})$$

From the convolution integral of $f(t)$ with $g_{in}(t)$ the signal at the detector, $g_{out}(t)$, can be calculated. A comparison of the functions g_{in} and g_{out} in Fig. 3 indicates that the peak shape is not perturbed by dispersion effects. This indicated that TPR profiles measured in our experimental arrangement had

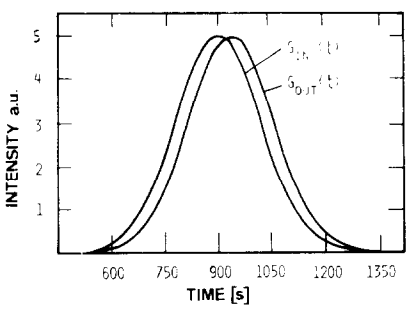

FIG. 3. Influence of the dispersion caused by the tubing between the reactor and the detector on the peak shape of a test peak.

to be corrected only for the time lag caused by the tubing.

To account for a possible time lag in the temperature measurement caused by the low thermal conductivity of the glass which separated the thermocouple from the reducing gas, temperature variations with constant heating rates were monitored both with the thermocouple arrangement used in the TPR experiments and, for comparison, with an arrangement in which the thermocouple was contacted directly with the reducing gas. From the observed steady-state temperature difference, the relaxation time (time to reach 63% of the final temperature when the system is subjected to a step change in temperature) of the temperature measurement was 20 s. Thus, the measured sample temperature, T_{meas}, had to be corrected for the time lags generated by the dead volume, V_t, and the non-zero response time of the temperature measurement according to the following correlation:

$$T = T_{meas} + \beta(\tau - V_t/V^*) \qquad (14)$$

Parametric Sensitivity

The observed sensitivity of the temperature, T_M, to a change in the operating variables is illustrated in Figs. 4A–D. For comparison the T_M values resulting from the integration of Eq. (5) with the estimated parameters k_0 and E_A are also included in these plots. By increasing the heating rate from 0.09 to 0.31 K/s T_M increases by 33 K. The slope of the curve decreases for increasing values of β. Since the integral hydrogen consumption is constant, the sensitivity of the method becomes lower for small heating rates indicating a proportionality to the heating rate. When the hydrogen concentration is increased from 3% (1.23 μmol/cm^3) to 15% (6.15 μmol/cm^3) T_M decreases from 604 to 563 K. From the measurements, it emerges that the sensitivity is inversely proportional to the hydrogen concentration in the feed.

A variation of the total flow rate in the range of 0.7 to 1.7 cm^3 (NTP)/s has only a small effect on the maximum temperature. For values of V^* below 0.7 cm^3 (NTP)/s,

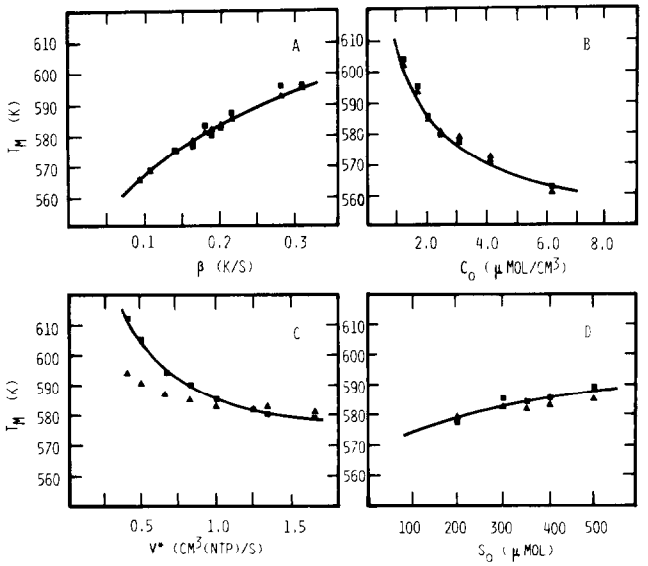

FIG. 4. Parametric sensitivity of the temperature of the maximum reduction rate. (A) Heating rate; (B) hydrogen concentration; (C) total flow rate; (D) amount of reducible species. Standard conditions: c_0 = 2.46 μmol/cm^3; S_0 = 405 μmol NiO; V^* = 1.25 cm^3 (NTP)/s; β = 0.2 K/s. (■) Measured values, (▲) calculated values.

there is, however, a weak accordance between the calculated and the experimental values. This behavior will be discussed in detail later. An increase in the sensitivity of the method is obtained by employing lower flow rates. A variation of the sample volume within an appropriate range causes only a minimal change in T_M as shown in Fig. 4D. The applied variation of the experimental parameters had no influence on the degree of reduction of the nickel oxide.

Estimation of Kinetic Parameters from Experiments with Variation of Different Operating Variables

Variation of the heating rate. For constant values of c_0, V^*, and S_0, three methods were applied to estimate the kinetic parameters k_0 and E_A. Method I refers to evaluation of the data by linear regression employing Eq. (8). Method II involves nonlinear regression and peak shape analysis for each TPR profile using Eq. (5). Method III is similar to Method II except that the regression analysis is carried out by employing all measured profiles simultaneously.

For analysis with Methods II and III the experimental profiles were divided into at least 20 data pairs $(T_i, (dn/dt)_i)$, uniformly distributed over the complete temperature range of the reduction. The parameters k_0 and E_A were then estimated by means of a computer program for multi-response algebraic and ordinary differential equation models (*15*). The residual sum of squares of the differences between the measured $(dn/dt)_{i,meas}$ and the calculated $(dn/dt)_{i,calc}$ values for the hydrogen consumption rates was chosen as the objective function.

$$RSS = \sum_{i=1}^{n} \left[\left(\frac{dn}{dt}\right)_{i,meas} - \left(\frac{dn}{dt}\right)_{i,calc} \right]^2 \quad (15)$$

A similar analysis has been reported by Tokoro *et al.* (16) for TPD profiles. These authors started with an algebraic model and calculated the current surface coverage with the experimental TPD curves assuming a total initial surface coverage. In contrast, our procedure starts directly with the differential equation (Eq. 5), and no assumptions have to be made about the measured profiles because all quantities in Eq. (5), except the kinetic parameters, are known or determined by the integration of the differential equation. The following kinetic parameters were obtained by analyzing data from runs 1–11 with Methods I and III, respectively (values in brackets are 95% confidence limits):

Method I:

$$E_M = 24;\ k_0 = 1.21 \times 10^{11}\ 1/(\text{mol} \cdot \text{s});\quad E_A = 117\ \text{kJ/mol}\ [101\text{–}133]$$

Method III:

$$E_M = 27;\ k_0 = 1.73 \times 10^{12}\ 1/(\text{mol} \cdot \text{s});\quad E_A = 129\ \text{kJ/mol}\ [127\text{–}131]$$

The experimental conditions and the values estimated with Method II are given in Table 2. The activation energies estimated agree fairly well with those reported in earlier investigations, where $E_A = 117$ kJ/mol was found if the experiments were started at initial conversions exceeding 10% (*17, 18*). Methods I and III do not yield significantly different activation energies. However, the confidence limits computed with Method III are narrower, mainly due to the large number of data points (more than 200 for the 11 experimental runs) used for the regression analysis. With Method I only the 11 experimental points at the peak maxima are used. All calculated T_M values were computed by numerical integration of Eq. (5) using the kinetic parameters obtained with Method III. Calculated and measured TPR profiles for four representative TPR experiments are compared in Fig. 5. At low temperature (start of reduction) a significant deviation between the measured and calculated profiles is observed. This behavior is ascribed to an induction period during which stable metal nuclei are formed on the surface of the oxide. After completion of the nucleation process, the only parameter

TABLE 2

TPR Experiments Performed with Different Heating Rates

Experiment	β (K/s)	$\bar{c}_M$ (μmol/cm^3)	T_M experimental (K)	T_M calculated (K)	$k_0 \times 10^{-13}$ (1/(mol · s))	E_A (kJ/mol)
1	0.17	1.98	576	578	0.66	134
2	0.28	1.73	595	592	0.26	131
3	0.09	2.18	565	565	1.42	138
4	0.22	1.87	587	584	0.95	137
5	0.14	2.07	575	574	3.28	142
6	0.14	2.05	575	574	1.67	139
7	0.31	1.68	596	594	0.08	125
8	0.11	2.14	568	568	0.38	132
9	0.20	1.90	582	583	0.47	133
10	0.18	1.96	583	580	0.22	131
11	0.19	1.94	580	582	0.81	135

Note. Conditions: c_0 = 2.46 μmol/cm^3; V^* = 1.25 cm^3 (NTP)/s; S_0 = 405 μmol NiO; K = 130 s.

governing the kinetics is the rate of the progression of the reaction zone.

For the TPR measurement No. 4 (see Table 2), the experimental profile was standardized using Eqs. (9) and (10), and the resulting curve was included in Fig. 2. In the range where $T_n < 0.95$, the measured hydrogen consumption rate is lower than the calculated one. Consequently, the experimental profiles appear to be sharper leading to higher values of E_M estimated by interpolation. Because the values of the hydrogen consumption rates at low conversions were also included in the peak shape analysis, slightly higher activation energies are expected to be found with Methods II and III. This trend is easily confirmed by comparing the values computed with the different methods.

A comparison of the measured and the calculated values of T_M (Table 2) and of the experimental and fitted TPR profiles (Fig. 5) leads to the conclusion that the effect of varying the heating rate on the TPR measurements can be described satisfactory by the model applied.

Variation of the hydrogen concentration. The change in the temperature T_M caused by a variation of the hydrogen concentration in the reducing gas between 1.23 and 6.15 μmol/cm^3 is illustrated in Fig. 4B. Experiments performed under the conditions listed in Table 3 were first analyzed using Eq. (8) (Method I). In a second step, the linear regression was carried out using also the experiments performed with different heating rates (Fig. 6). The following kinetic parameters were estimated (values in brackets are 95% confidence limits):

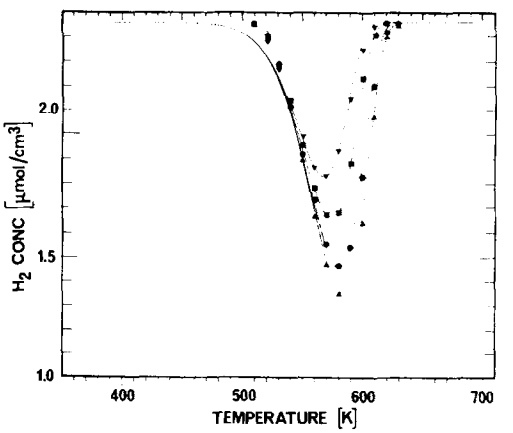

FIG. 5. Comparison of measured and calculated TPR profiles for experiments with different heating rates. Calculation based on kinetic parameters obtained with method III. Conditions: S_0 = 405 μmol NiO; V^* = 1.25 cm^3 (NTP)/s; c_0 = 2.46 μmol/cm^3. Heating rates: (▼) 0.11 K/s (Exp. 8); (■) 0.14 K/s; Exp. 6); (●) 0.18 K/s (Exp. 10); (▲) 0.20 K/s (Exp. 9).

Profiles 11–17: $E_M = 26$;
$k_0 = 5.61 \times 10^{11}$ 1/(mol · s);
$E_A = 124$ kJ/mol [106–142]

Profiles 1–17: $E_M = 25$;
$k_0 = 3.34 \times 10^{11}$ 1/(mol · s);
$E_A = 121$ kJ/mol [110–132]

By applying Eq. (8) no significant difference can be found between the kinetic parameters estimated from experiments where the hydrogen concentration was varied or from those where the heating rate was varied. The confidence limits for the estimated parameters decrease, of course, by using more experimental runs. In our case, at least 10 profiles have to be used to compute reliable kinetic parameters. However, even when using all experimental runs (runs 1–17) for the linear regression analysis, such narrow confidence limits as found with Method III were not obtained.

The experimentally observed changes in T_M are reasonably described by the values computed by the integration of Eq.(5) using the kinetic parameters estimated with Method III. For low hydrogen concentrations ($c_0 < 3$ μmol/cm^3) in the reducing gas, the sensitivity of the T_M values is increased (Fig. 4B).

Variation of the total flow rate and of the amount of sample. The model applied to the TPR measurements is based on the simplifying assumption that the mean hydrogen concentration between reactor inlet and outlet is the driving force for the reduction. The validity of this assumption is only met with low fractional conversions of the hydrogen. On the other hand, the difference of the hydrogen concentration between reactor inlet and outlet must be detectable. In particular, the detector signal due to the change in hydrogen concentration has to be large compared to the statistical noise of the baseline.

The following criteria may help to meet these requirements: (A) The amount of hydrogen consumed at the peak maximum should not exceed $\frac{2}{3}$ of the hydrogen feed to the reactor [$C_M > 0.33 \cdot C_0$]; (B) The minimum conversion at the peak maximum should be 10% [$C_M < 0.9\ C_0$].

For experimentally relevant heating rates between 0.1 and 0.3 K/s and known reduction kinetics, it is possible to compute sets of the operating variables (β, S_0, c_0, V^*) which meet criteria A and B. Figure 7 shows the result of such a consideration. For different heating rates, the molar hydrogen flux leaving the reactor at $T = T_M$ is plotted as a function of the amount of sample. Experimental conditions within the rectangular area meet criteria A and B. A characteristic number, K, may be defined to facilitate the selection of appropriate operating variables.

$$K = \frac{S_0}{V^* c_0} \tag{16}$$

TABLE 3

TPR Experiments Performed with Different Hydrogen Concentrations

Experiment	K (s)	β (K/s)	c_0 (μmol/cm^3)	$\bar{c}_M$ (μmol/cm^3)	T_M experimental (K)	T_M calculated (K)
12	156	0.20	2.05	1.53	585	586
13	104	0.22	3.08	2.47	577	579
14	78	0.22	4.11	3.46	571	573
15	52	0.20	6.16	5.49	563	561
16	260	0.20	1.23	0.77	604	603
17	195	0.22	1.64	1.13	596	596

Note. Conditions: $V^* = 1.25$ cm^3 (NTP)/s; $S_0 = 405$ μmol NiO.

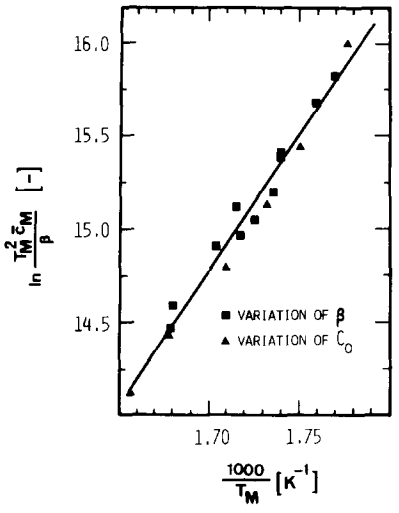

FIG. 6. Experiments with variation of the heating rate and hydrogen concentration evaluated by linear regression according to Eq. (8). For conditions see Tables 2 and 3.

The minimum value of K is 55 s for a heating rate of 0.1 K/s (criterion B), and the maximum value is 140 s for β = 0.3 K/s (criterion A). For values of K below 55 s the sensitivity becomes too low; for values of K exceeding 140 s, the quantity of hydrogen consumed is too large, resulting in a violation of the assumption of a linear concentration profile. The operating variables can easily be optimized either by calculating the factor K or by preparing such diagrams as shown in Fig. 7. A possible extension is to perform experiments, giving the same hydrogen consumption rate at the peak maximum; for example, this may be done by appropriately varying the heating rate together with the amount of reducible species.

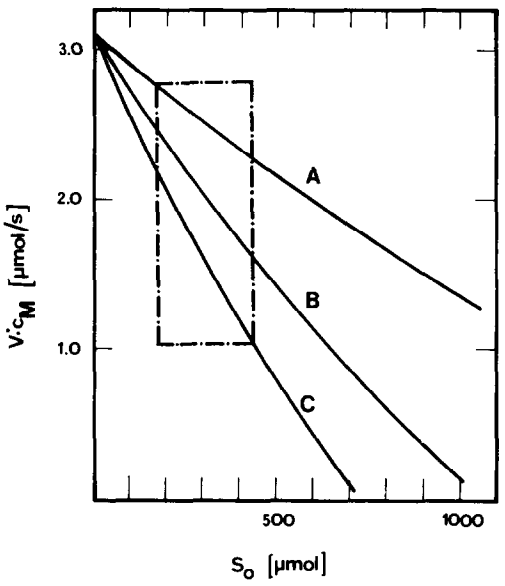

FIG. 7. Minimum molecular hydrogen flow rate at the reactor outlet calculated for different heating rates ((A) 0.1 K/s, (B) 0.2 K/s, (C) 0.3 K/s) and amounts of reducible sample. Operating conditions within the rectangular area meet criteria A and B. Conditions: c_0 = 2.46 μmol/cm³; V^* = 1.25 cm³(NTP)/s.

The experimentally observed effect of the variation of the total flow rate on the temperature T_M and the corresponding curve are shown in Fig. 4C. Differences of more than 10 K between measured and calculated values were found for flow rates smaller than 0.7 cm³ (NTP)/s. If the total flow rate goes down, the TPR profiles become broader (see $B_{1/2}$ in Table 4). However, in experiments carried out with reasonable values for K (see Table 4), a good accordance of experimental and simulated values of T_M is found. The deviation found between the experimental and calculated curve (Fig. 4C) cannot be explained by mass transfer influences, as will be shown later. Two effects are responsible for the deviation between experimental and calculated profiles at low flow rates. The first is the appreciable time lag for the temperature measurement and the second is an increase in dispersion effects, both due to low flow rates. For experiments with low flow rates, the characteristic number K reaches values up to 390 s, and criterion A is severely violated. This shows the importance of careful selection of experimental parameters in order to obtain consistent results.

In an appropriate range (K values: 65–162 s) a variation in the amount of reducible species changes the temperature of the maximum reduction rate by only 10 K. With the conditions given in Table 5, a good fit between experimental and calculated values of T_M is obtained (Fig. 4D). The total

TABLE 4

TPR Experiments Performed with Different Flow Rates of the Reducing Gas

Experiment	K (s)	β (K/s)	V^* (cm³(NTP)/s)	T_M experimental (K)	T_M calculated (K)	$B_{1/2}$ (K)
9	130	0.20	1.25	582	583	56
18	122	0.21	1.33	580	584	59
19	163	0.19	1.00	586	583	63
20	244	0.20	0.67	594	588	68
21	325	0.19	0.50	605	591	74
22	192	0.20	0.83	590	585	66
23	390	0.20	0.42	612	594	85
24	97	0.21	1.67	579	582	53

Note. Conditions: c_0 = 2.46 μmol/cm³; S_0 = 405 μmol NiO.

flow rate and the amount of sample do not appear in Eq. (8) which is the basic equation for the quantitative analysis of TPR data. For constant heating rate and initial hydrogen concentration, the hydrogen concentration at the exit of the reactor is lower for increasing values of S_0 or decreasing values of V^*. Consequently, the mean hydrogen concentration and the reduction rate are decreased and the recorded TPR profiles are shifted to higher temperatures.

Mass Transfer Limitations in TPR Experiments

The shape of reduction profiles can be influenced by mass transfer effects. It is therefore of major importance to check whether the measurements are free from inter- and intraparticle mass transfer limitations. A possible procedure to check for mass transfer effects will subsequently be described using an alumina-supported copper catalyst as an example. The criterion is based on experiments conducted with catalyst samples of different particle sizes. Measurements performed under standard conditions did not indicate any significant change in the peak shape or in the temperature of the maximum reduction rate, showing that our measurements were free from intraparticle mass transfer limitations (see Table 6). If the physical properties of the sample and the hydrogen consumption rate at the peak maximum are known, the TPR measurement can be checked for mass transfer limitations applying the procedure given below.

TABLE 5

TPR Experiments Performed with Different Amounts of Reducible Species

Experiment	K (s)	β (K/s)	S_0 (μmol)	T_M experimental (K)	T_M calculated (K)
25	65	0.20	199	578	580
26	99	0.21	305	586	583
27	114	0.21	349	585	583
28	130	0.21	400	587	584
29	163	0.22	500	590	586

Note. Conditions: c_0 = 2.46 μmol/cm³; V^* = 1.25 cm³ (NTP)/s.

Interparticle mass transfer limitation. For mass transfer in fixed and fluidized beds Gunn (*19*) derived the correlation:

$$Sh = \frac{2k_f R_p}{D} = (7 - 10\varepsilon + 5\varepsilon^2)(1 + 0.7Re_p^{0.2}Sc^{1/3}) + (1.33 - 2.4\varepsilon + 1.2\varepsilon^2)Re_p^{0.7}Sc^{1/3} \quad (17)$$

The experimental values for the Reynolds numbers in our measurements were between 0.06 and 1 (see Table 6). For mass

TABLE 6

Test for Significance of Inter- and Intraparticle Diffusion Effects in the Reduction of Alumina-Supported Copper Oxide

Experiment	$\bar{R}_p$ (cm)	Re_p	T_M (K)	$\left(\frac{dn}{dt}\right)_M$ (μmol/s)	Φ	$\frac{c_0 - c_s}{c_0} \times 10^2$
31	0.035	0.30	543	1.12	0.27	0.0200
32	0.015	0.10	544	1.17	0.05	0.0037
33	0.0075	0.06	542	1.10	0.01	0.0009

Note. Conditions: β = 0.2 K/s; c_0 = 2.46 μmol/cm^3; V^* = 1.25 cm^3 (NTP)/s; S_0 = 400 mg; K = 127 s.

transfer by bulk diffusion in a bed of porosity $\varepsilon = 0.4$, a limiting value of 3.8 for the Sherwood number is obtained. The concentration gradient between the particle surface and the bulk gas phase is calculated by employing Eq. (18).

$$\left(\frac{dn}{dt}\right)_M = k_f A(c_0 - c_s) = 1.9\frac{D}{R_p}A(c_0 - c_s) \quad (18)$$

The total outer exchange surface, A, was determined from the sample weight and the apparent density, assuming spherical geometry for the particles. For the binary bulk diffusion coefficient, $D = D_{H_2,N_2}$ a value of 1.69 cm^2/s (*21*) was used. Values estimated for the quantity $(c_0 - c_s)/c_0$ are less than 1%. Thus we conclude that interparticle diffusion limitations have no influence on the reduction rates measured in our TPR experiments.

Intraparticle diffusion limitation. Ibok and Ollis (*20*) presented a simple criterion for checking pore diffusion limitations in TPD experiments. The same analysis can be performed for TPR experiments. The criterion is based on the dimensionless number Φ defined in Eq. (19).

$$\Phi = \frac{R_p^2}{D_{eff}}\left(\frac{1}{V_c}\left(\frac{dn}{dt}\right)_M\right)\frac{1}{c_s} \quad (19)$$

If the values found for Φ are less than 0.3, it is concluded that no appreciable diffusion gradients exist within the pellet. The Φ values calculated for our experiments are listed in Table 6. These values were obtained with $(dn/dt)_M$ = 1.13 μmol/s and D_{eff} = 1.4 × 10^{-2} cm^2/s. Transition region diffusion was assumed for the evaluation of D_{eff} and a value of 3 was chosen for the tortuosity factor. The volume, V_c, was calculated from the apparent density of the sample.

A critical particle radius can be estimated by introduction of the limiting value Φ = 0.3 into Eq. (19). According to this estimate, experiments with particles having radii of 0.04 cm or less are not expected to be influenced by intraparticle mass transfer limitations, under the experimental conditions given. The experimental results summarized in Table 6 confirm the validity of the criterion of Eq. (19). No general upper limit for the dimension of the particles can be given. It is proposed to check for possible mass transfer limitations either with appropriate experiments or by using Eqs. (18) and (19) for a preliminary evaluation.

CONCLUSION

The effect of the different operating variables used in TPR experiments on the reduction profiles obtained has been investigated using the reduction of nickel oxide as an example. The heating rate and the hydrogen concentration in the reducing gas were found to have a more pronounced effect on the temperature of the maximum reduction rate than the total flow rate or the

amount of reducible sample. The observed effects of the different operating variables demonstrate that optimal results with respect to sensitivity can only be obtained if the operating variables are properly selected. For this purpose a characteristic number, K, is defined to facilitate selection of an appropriate set of operating variables.

$$K = \frac{S_0}{V^* \cdot c_0} \qquad (16)$$

For commonly used heating rates between 0.1 and 0.3 K/s, the limiting values are $55 < K < 140$ s. According to Eq. (16) improved sensitivity of the TPR method is obtained by using low feed rates ($V^* \cdot c_0$) of hydrogen. The total flow rate is the parameter which dominantly influences the time lag of the temperature measurement and the dispersion of the original signal between reactor and detector. These effects become more important if the selected flow rates are low. Thus, for the quantitative analysis of TPR data, it is indispensable to consider these effects quantitatively; small errors in the determination of the temperature of the maximum reduction rate and of the TPR peak shape can lead to appreciable errors in the estimated kinetic parameters (*14*).

A method for estimating kinetic parameters by means of total peak shape analysis was applied to the TPR profiles measured for the nickel oxide. Similar kinetic parameters were obtained from estimations where only the temperature of the maximum hydrogen consumption rate was used for the analysis. However, the confidence limits for the kinetic parameters were significantly narrower when using a complete peak shape analysis.

For measurements in which the operating variables were optimized good accordance was obtained between measured reduction profiles and profiles simulated using the kinetic parameters estimated by a peak shape analysis.

Criteria for estimating inter- and intraparticle diffusion limitations in TPR experiments have been proposed and applied to the reduction of alumina-supported copper oxide particles of different size.

ACKNOWLEDGMENT

The Swiss National Science Foundation is gratefully acknowledged for financially supporting this work (Project: 2.806-0.80).

REFERENCES

1. Robertson, S. D., McNicol, B. D., De Baas, J. H., and Kloet, S. C., *J. Catal.* **37,** 424 (1975).
2. Gentry, S. J., and Walsh, P. T., *J. Chem. Soc. Faraday Trans. I* **78,** 1515 (1982).
3. Jacobs, P. A., Linart, J., Nijs, H., and Uytterhoeven, J. B., *J. Chem. Soc. Faraday Trans. I* **73,** 1745 (1977).
4. Wagstaff, N., and Prins, R., *J. Catal.* **59,** 434 (1979).
5. Isaacs, B. H., and Petersen, E. E., *J. Catal.* **77,** 43 (1982).
6. Lycourghiotis, A., Defosse, C., Delannay, F., Lemaitre, J., and Delmon, B., *J. Chem. Soc. Faraday Trans. I* **76,** 1677 (1980).
7. Gentry, S. D., Hurst, N. W., and Jones, A., *J. Chem. Soc. Faraday Trans. I* **77,** 603 (1981).
8. McCarty, J. G., and Wise, H., *J. Catal.* **57,** 406 (1979).
9. Hurst, N. W., Gentry, S. J., Jones, A., and McNicol, B. D., *Catal. Rev.* **24,** 233 (1982).
10. Gentry, S. J., Hurst, N. W., and Jones, A., *J. Chem. Soc. Faraday Trans. I* **75,** 1688 (1979).
11. Best, R. J., and Russell, W. W., *J. Am. Chem. Soc.* **76,** 838 (1954).
12. Baiker, A., and Richarz, W., *Synth. Commun.* **8,** 27 (1978).
13. Cvetanović, R. J., and Amenomiya, Y., *in* "Advances in Catalysis" (D. D. Eley, H. Pines, and P. B. Weisz, Eds.), Vol. 17, p. 103. Academic Press, New York, 1967.
14. Brenner, A., and Hucul, D. A., *J. Catal.* **56,** 134 (1979).
15. Klaus, R., and Rippin, D. W. T., *Comput. Chem. Eng.* **3,** 105 (1979).
16. Tokoro, Y., Uchijima, T., and Yoneda, Y., *J. Catal.* **56,** 110 (1979).
17. Delmon, B., *Bull. Soc. Chim. Fr.* **1961,** 590 (1961).
18. Delmon, B., *in* "Introduction à la Cinétique Hétérogène." Editions Technip, Paris, 1969.
19. Gunn, D. J., *Int. J. Heat Mass Transfer* **21,** 467 (1978).
20. Ibok, E. E., and Ollis, D. F., *J. Catal.* **66,** 391 (1980).
21. Reid, C. R., Prausnitz, J. M., and Sherwood, T. K., *in* "The Properties of Gases and Liquids," 3rd ed., McGraw–Hill, New York, 1977.